VNU Journal of Science: Mathematics – Physics, Vol. 30, No. 2 (2014) 10-17

Segregation of Manganese Atoms during the Growth of $Ge_{1-x}Mn_x$ Nanocolumns on Ge (001)

Le Thi Giang, Nguyen Manh An*

Hong Duc University, 565 Quang Trung, Thanh Hoa, Vietnam

Received 20 May 2014
Revised 19 June 2014; Accepted 27 June 2014

Abstract: High resolution - transmission electron microscopy (HR-TEM), along with Reflection High-Energy Electron Diffraction (RHEED) and Laser pulse atom probe tomography (LP- APT) were used to investigate the growth kinetics of $Ge_{1-x}Mn_x$ nanocolumn on Ge(001) and the mechanism of $Ge_{1-x}Mn_x$ nanocolumn formation. The results evidence that during the deposition of $Ge_{1-x}Mn_x$ film, Mn atoms diffuse into the Ge matrix to form Mn-rich regions and the upward segregation of Mn atoms along the [001] direction is the origin of the Mn concentration enrichment inside the nanocolumns.

Keywords: Diluted magnetic semiconductors, nanocolumns, Ge_3Mn_5 clusters, Mn segregation.

1. Introduction

In the past few years, the synthesis of ferromagnetic semiconductors has become a major challenge for spintronics. Actually, growing a magnetic and semiconducting material could lead to promising advances such as spin injection into nonmagnetic semiconductors, or electrical manipulation of carrier-induced magnetism in magnetic semiconductors [1,2]. Up to now, major efforts have focused on diluted magnetic semiconductors (DMS) in which the host semiconducting matrix is randomly substituted by transition metal (TM) ions such as Mn, Cr, Ni, Fe, or Co [3]. However, Curie temperatures (T_C) of DMS remain rather low and TM concentrations must be drastically raised in order to increase T_C up to room temperature. This process usually combines with the phase separation and the formation of secondary phases. The origin of this phenonmenon probably arises from a very low solubility of TM atoms in the semiconducting matrix.

The increasing interest in group-IV magnetic semiconductors can also be connected to their potential compatibility with the existing silicon technology. $Ge_{1-x}Mn_x$ DMS would be a potential candidate, since it can easily be integrated into semiconductor hetero-structures. Moreover, the spin injection from $Ge_{1-x}Mn_x$ DMS is expected to be highly efficient thank to the natural impedance match

* Corresponding author. Tel: 84-903296502.
E-mail: nguyenmanhan@hdu.edu.vn

to Ge [4-6]. Different kinds of embedded Mn-rich phases have been identified, such as Mn-rich elongated structures [7], amorphous Mn-rich precipitates [8], self-assembled nanocolumns [9]. However, the most favourable candidate is the metallic Ge_3Mn_5 clusters [10-12]. For spintronic applications, the nanocolumn structure appears particularly interesting, because it exhibits semiconducting conductivity and remains ferromagnetic up to temperatures above 400 K and [9]. The composition of this nanocolumn phase has been attributed to be close to a Ge_2Mn compound, which does not exist in the Ge-Mn phase diagram[13]. The formation of the defined compound with homogeneous concentration through whole the length of a nanocolumn and the significant increase of T_C in nanocolumns [9, 15] can be explained by Fukushima *et al.*,[14]. In this model, the phase separation is described by two-dimensional spinodal decomposition in the growth direction. While being fascinated by this finding, the kinetic formation of this nanocolumn phase is still interesting to exame.

In this work, we report the mechanism of the formation of $Ge_{1-x}Mn_x$ nanocolumn phase. The model concern to the lateral segregation of Mn atoms in Ge matrix due to the low solubility of Mn atoms in Ge matrix and the vertical segregation of Mn atoms due to the sub-surfactant effect of Mn atoms during the deposition of $Ge_{1-x}Mn_x$ film on Ge(001) substrate [16, 17].

2. Experimental

$Ge_{1-x}Mn_x$ films were grown by molecular beam epitaxy (MBE) on epi-ready n-type Ge(001) wafers with a nominal resistivity of 10 Ω.cm at CINaM (Centre Interdisciplinaire de Nanosciences de Marseille, France). The base pressure in the MBE system is better than 5 x 10^{-10} Torr. The growth chamber is equipped with a reflexion high-energy electron diffraction (RHEED) technique to control the cleanness of the substrate surface prior to growth and to monitor the epitaxial growth process. $Ge_{1-x}Mn_x$ films were obtained by co-deposition of Ge and Mn from standard Knudsen effusion cells. The Ge deposition rate was determined from RHEED intensity oscillations whereas the Mn deposition rate was deduced from Rutherford backscattering spectrometry (RBS) measurements. The standard growth rate used in this work is of 1 – 2 nm/min.

The cleaning of Ge(001) surfaces was carried out in two steps: a chemical cleaning to remove hydrocarbon related contaminants followed by an in-situ thermal cleaning at ~750°C to remove Ge surface oxide layers. After this step, the Ge(001) surface generally exhibits a (2×1) reconstruction. To insure a good starting Ge surface prior to $Ge_{1-x}Mn_x$ growth, a ~ 30-50 nm thick Ge buffer layer was systematically grown at a substrate temperature of 400°C. Fig. 1a and b respectively display RHEED patterns taken along the $[1\bar{1}0]$ and [100] azimuth of the clean Ge surface prior to $Ge_{1-x}Mn_x$ growth. The Ge surface is characterized by a well-developed 2×1 streaky pattern, indicating that the surface is clean and smooth. This is also confirmed by the observation of high-intensity Kikuchi lines, which overlap *1*×1 and specular streaks, giving rise to localized reinforcements of intensity, as can be seen in RHEED patterns.

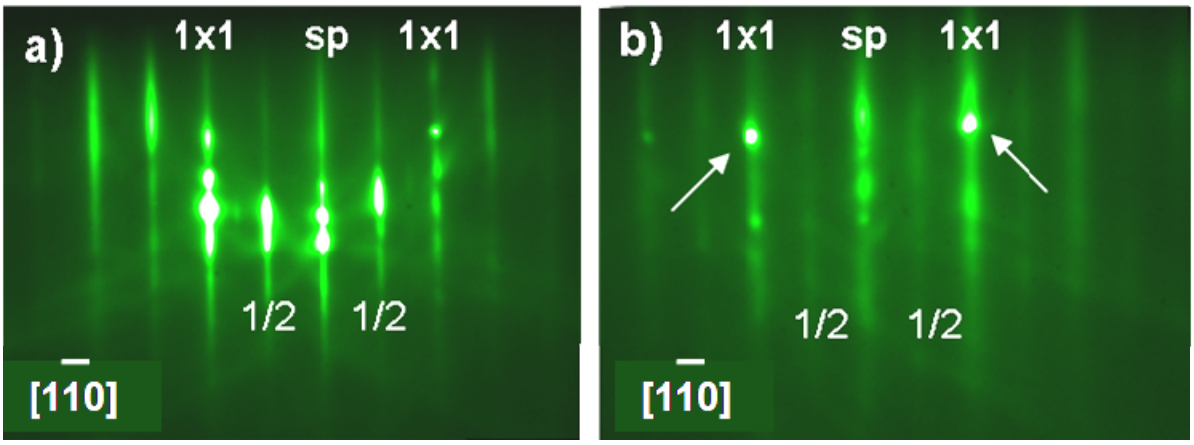

Figure 1. RHEED patterns taken along the [1$\bar{1}$0] and [100] azimuth of the clean Ge surface.

Structural analyses of the grown films were performed through extensive high resolution transmission electron microscopy (TEM) by using a JEOL 3010 microscope operating at 300 kV with a spatial resolution of 1.7 Å. Particularly, the Laser Pulse Atom Probe Tomography (LP-APT) technique was set up to determine at atomic scale the gradient of Mn composition inside nanocolumns. LP-APT measurements were performed using an Imago LEAP 3000X HR microscope in the pulsed laser mode. The analyses were carried out at 20.3 K, with a laser pulse frequency of 100 kH.

3. Results and discussion

As we have shown in the previous studies, under specific conditions of growth temperature and Mn concentration, epitaxial growth of GeMn alloys on Ge(001) substrates can be resulted in the formation of nanocolumns, which are orientated along the growth direction and entirely coherent with the surrounding diluted matrix. We have provided, for the first time, that the Mn concentration in nanocolumns is highly inhomogeneous, not only along the growth direction but also parallel to it due to the core-shell structure [18-21]. To understand the variation of the Mn concentration in $Ge_{1-x}Mn_x$ nanocolumns, we attempt, in this paper, to provide a phenomenological explanation of the $Ge_{1-x}Mn_x$ nanocolumn formation.

The Mn concentration inside nanocolumns can be demonstrated by LP-APT measurements. That is a three-dimensional useful technique in analysis of subsurface or buried features in specimens with very high sensitivity. The high spatial resolution of the technique makes it especially practical in the investigation the size, the composition, the morphology, and the evolution of the solute segregation [22]. Indeed, the evidences of the Mn concentration gradient in the nanocolumns by an extension of the iso-concentration series in 3D reconstruction is presented in Figure 2 for the Mn concentration (C_M) of 5, 15 to 25 %. It can be seen from this figure that the nanocolumn reconstructions near the interface decrease with increasing C_M. At the Mn concentration of 5% which is much lower level than

average Mn content inside the nanocolumn, the whole nanocolumns are presented from the interface to the surface. For C_M= 15%, a slightly change is observed at the layer closed to the surface. The cores of the nanocolumns are visible near the interface only. At high Mn concentration of 25%, the nanocolumns near the interface are almost disappeared. Only some of nanocolumns cores close to the surface still remain. These results reflect the fact that Mn concentration gradient in nanocolumns exist not only along the growth direction, but also through the nanocolumns, from column shell to the core. These findings reinforce that the nanocolumns are not form by the Ge_2Mn intermetallic compound as reported in ref. 9,14,15 but by a $Ge_{1-x}Mn_x$ solid solution.

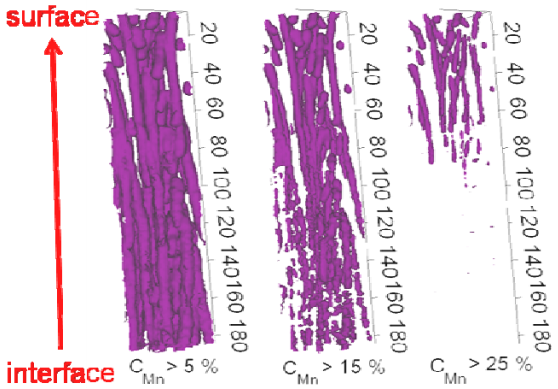

Figure 2. Iso-concentration surfaces made of the same volume for three different Mn concentrations 5, 15 and 25 %.

To understand the mechanism of the nanocolumn formation, we first recall that under non-equilibrium growth carried out at a temperature as low as 130 °C the Ge lattice can dilute a Mn concentration of about 0.25 to 0.5 %. When the first monolayers of GeMn alloys with Mn concentration as high as 4-7% (condition for nanocolumn formation) are deposited on a Ge surface, excess Mn should diffuse and/or segregate along the surface to form Mn-rich regions. Differently speaking, Mn-rich regions start to nucleate on the surface even after deposition of the first monolayers and this is a direct consequence of the low solubility of Mn in the Ge lattice.

The formation of such Mn-rich regions on the surface should 'disturb' the surface morphology. This is what we have observed from RHEED patterns during the very early growth stage of GeMn alloys. Fig. 3 shows the evolution of RHEED patterns upon the deposition of the first monolayers of GeMn. Prior to GeMn deposition, the Ge surface exhibits a well-defined 2×1 reconstructed RHEED pattern (Fig. 3a). As soon as growth starts, 2×1 ordered streaks disappear, leaving a 1×1 pattern (Fig. 3b). Probably, the presence of Mn-rich nuclei is responsible for this change since a very diluted GeMn alloy (with Mn content of 0.25 - 0.5 %) should display a 2×1 and two-dimensional RHEED pattern. Since a too high Mn concentration in a nucleus is not favorable, both from the thermodynamical and epitaxial points of views, the system should self-organize to form nuclei with a certain density. Note that the size and the interdistance between nuclei should depend on the Mn diffusion length, i.e., the substrate temperature. We display in Fig. 3c a schema illustrating the formation of these Mn-rich

nuclei on the Ge surface. When the GeMn deposition proceeds, these nuclei may serve as seeds for the nanocolumn formation.

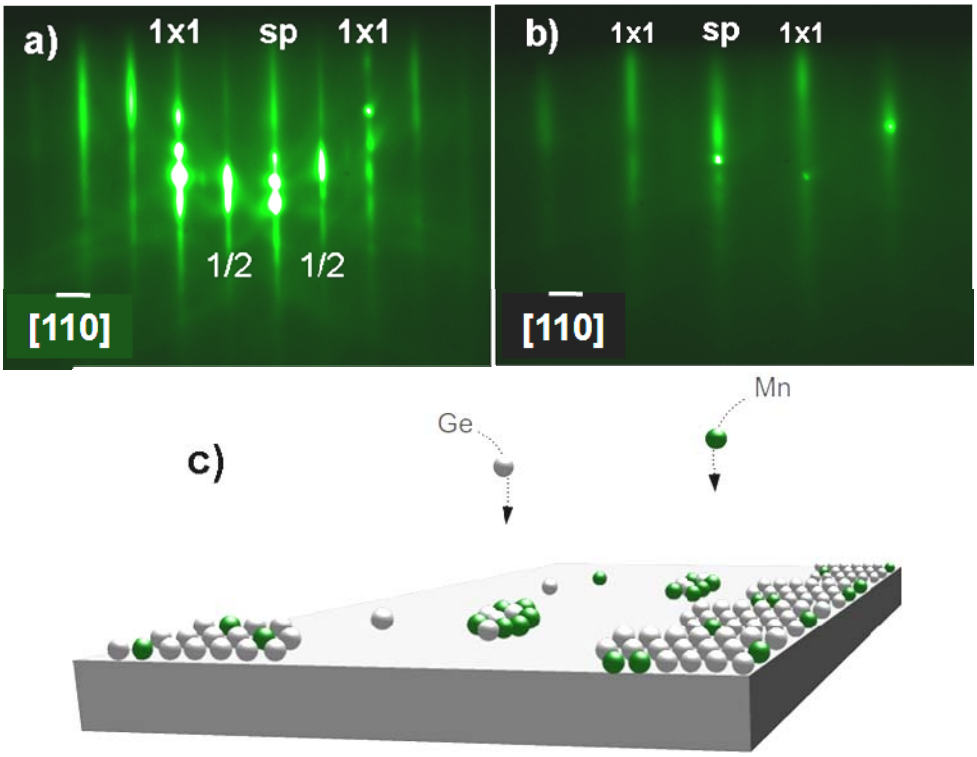

Figure 3. RHEED patterns taken along the [1$\bar{1}$0] azimuth of a clean Ge surface prior to growth (a), during the growth of the first monolayers (b). Schema illustrating the nucleation of Mn-rich regions on a Ge(001) surface due to a low solubility of Mn in Ge (c).

On the other hand, the increase of the Mn concentration within nanocolumns can be explained by vertical segregation of Mn along the [001] direction. Indeed, it has been shown using spin-polarized density functional theory (DFT) calculations that along the Ge(001) orientation, Mn atoms have tendency to float upwards the growth front via interstitial sites, acting thus as 'surfactants' [16, 17]. Based on this surfactant effect of Mn atoms, we can suggest that once Mn-rich nuclei are formed on the surface in the early stage of the growth, further deposition leads to the formation of columns in which the Mn concentration continuously increases due to the surfactant action of Mn atom along the [001] direction. We display in Fig. 4 a schema illustrating nanocolumns grow from initial Mn-rich nuclei on the surface. It is worth noting that the cylindrical shape of nanocolumns allows them to minimize their interface energy with the surrounding diluted matrix. This suggestion also implies that not all nanocolumns nucleate from the interface and across the whole layer. Depending on the Mn concentration in the top of nanocolumns, nanocolumn growth can be interrupted. In the same time, other nancolumns can start to nucleate in the middle of the layer if these regions are rich enough in Mn to form new nuclei. Similar results were observed from TEM analyses shown in ref. 18 and ref. 19.

In addition, as has been discussed in ref. 20, another interesting feature is the core-shell structure of nanocolumns. The results show that the nanocolumns exhibit a core-shell structure with a much higher Mn concentration in the core compared to that of the shell and Mn concentration in the matrix surrounding nanocolumns is much less variable with an *average* value of ~0.5%.

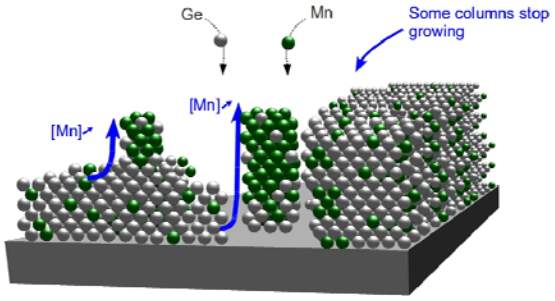

Figure 4. Schema illustrating the growth of nanocolumns from Mn-rich nuclei formed on the surface. Mn atoms are shown to float upward to the top of nanocolumns. The cylindrical shape of nanocolumns allows them to minimize their interface energy with the surrounding matrix.

Since the atomic radius of Mn atoms are slightly larger than that of Ge (127 and 122 picometers for Mn and Ge atoms, respectively), if the Mn concentration inside nanocolumns is too high, nanocolumns may exert a tensile train to the surrounding lattice. To reduce such a strain, a core-shell structure with a reduced Mn concentration from core to shell should allow nanocolumns to more easily adapt the lattice parameter of the surrounding lattice. Thanks to this self-organized core-shell structure, almost all nanocolumns are found to be perfectly coherent with the surrounding lattice, as can be seen in Fig. 1c and 1d of ref. 20.

To study the effect of the substrate orientation and in particular to verify the assumption of the 'surfactant' effect of Mn atoms along [001] direction of Ge, we have performed $Ge_{1-x}Mn_x$ growth on Ge(111) substrates. For GeMn-based materials, up to now Ge(111) substrates are mainly used for epitaxial growth of the Mn_5Ge_3 compound, which has a hexagonal symmetry similar to a three-fold symmetry of Ge(111) [23, 24]. Fig. 5a shows a typical TEM image of 80-nm-thick GeMn film grown on a Ge(111) substrate. We note that the growth temperature is 130^0C and the Mn concentration is about 6%, i.e., at the same growth conditions for $Ge_{1-x}Mn_x$ nanocolumns on Ge(001). The image clearly indicates that no nanocolumns are formed in the layers as in the case of GeMn growth on Ge(001). Phase separation due to a high Mn concentration in the Ge lattice does occur but Mn-rich 'regions' are organized along separated *streaks* that are not oriented along the growth direction but along the [110] direction. A detailed view of these streaks are presented in a HR-TEM image shown in Fig. 5b. It appears that the Mn-rich streaks organize within two pseudo-periodities: invidual streaks are separated by a periodicity of ~1nm and they form groups, which are separated one from the other by a periodicity of ~12 nm. We also note that the layer is relatively defected. The above results indicate that the nucleation of Mn-rich seeds on Ge(111) is different compared to that on Ge(001) and Mn segregation does not occurs along the [111] direction, which, according to energetic calculations [16], is not favorable.

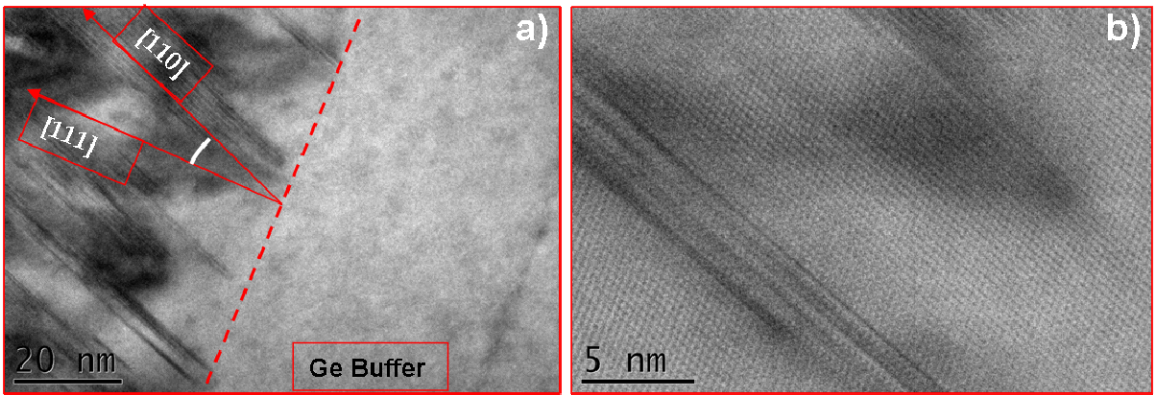

Figure 5. Typical TEM images of the 80-nm-thick $Ge_{0.94}Mn_{0.06}$ film grown on Ge(111) at 130 °C (a) and a detailed view of Mn-rich streaks observed inside the layer (b). The Mn-rich streaks form an angle α ~20 ^{o} to the growth direction.

4. Conclusion

The nanocolumn formation of $Ge_{1-x}Mn_x$ one have been described using a phenomenological model based on a three dimension Mn segregation (i. e. the segregation both in-plane and along the growth direction). The in-plane or lateral Mn segregation is driven by a low solubility of Mn in Ge while the driving force of Mn vertical segregation is induced by the surfactant effect along the [001] direction. Experiments of GeMn growth on Ge(111) surfaces seems to support the surfactant effect of Mn, which floats upward the growth front along the [001] direction.

Acknowledgments

This work was supported by the National Foundation for Science and Technology Development (NAFOSTED) under grant number of **103.02-2013.66**. The authors would like to thank Prof. Vinh LE THANH and Dr. Minh Tuan DAU - Centre Interdisciplinaire de Nanoscience de Marseille (CINaM-CNRS), France for their help.

References

[1] H. Ohno, D. Chiba, F. Matsukura, T. Omiya, E. Abe, T. Dietl, Y. Ohno, and K. Ohtani, Nature (London) 408 (2000), 944.
[2] H. Boukari, P. Kossacki, M. Bertolini, D. Ferrand, J. Cibert, S. Tatarenko, A. Wasiela, J. A. Gaj, and T. Dietl, Phys. Rev. Lett. 88 (2002), 207204.
[3] T. Dietl, Semicond. Sci. Technol. 17 (2002), 377.
[4] Y. D. Park, A. T. Hanbicki, S. C. Erwin, C. S. Hellberg, J. M. Sullivan, J. E. Mattson, T. F. Ambrose, A. Wilson, G. Spanos, and B. T. Jonker, Science 295 (2002), 651.
[5] A. Stroppa, S. Picozzi, and A. Continenza and A. J. Freeman, Phys. Rev. B 68 (2003), 155203.

[6] N. Pinto, L. Morresi, M. Ficcadenti, R. Murri, F. D'Orazio, F. Lucari, L. Boarino, and G. Amato, Phys. Rev. B 72 (2005), 165203.

[7] D. Bougeard, S. Ahlers, A. Trampert, N. Sircar, and G. Abstreiter, Phys. Rev. Lett. 97, 237202 (2006); S. Ahlers, D. Bougeard, N. Sircar, G. Abstreiter, A. Trampert, M. Opel and R. Gross, Phys. Rev. B 74 (2006), 214411.

[8] D. Bougeard, N. Sircar, S. Ahlers, V. Lang, G. Abstreiter, A. Trampert, J. M. LeBeau, S. Stemmer, D. W. Saxey, and A. Cerezo, NanoLetters 9 (2009), 3743.

[9] (a) M. Jamet, A. Barski, T. Devillers, V. Poydenot, R. Dujardin, P. Bayle-Guillemaud, J. Rothman, E. Bellet-Amalric, A. Marty, J. Cibert, R. Mattana, S. Tatarenko, Nat. Mater.5 (2006), 653.

[10] Y.D. Park, A. Wilson, A.T. Hanbicki, J.E. Matteson, T. Ambrose, G. Spanos, B.T. Jonker, Appl. Phys. Lett. 78 (2001), 2739.

[11] A.P. Li, J. Shen, J.R. Thompson, H.H. Weitering, Appl. Phys. Lett. 86 (2005), 152507.

[12] C. Bihler, C. Jaeger, T. Vallaitis, M. Gjukic, M.S. Brandt, E. Pippel, J. Woltersdorf, U. Gosele, Appl. Phys. Lett. 88 (2006), 112506.

[13] T.B. Massalki, Binary alloy phase diagrams, 2nd Edition, Vol 1, 2, ASM International 1992.

[14] Thesis of T. Devillers, Etude des propriétés physiques des phases de Ge1−xMnx ferromagnétiques pour l'électronique de spin, 2009.

[15] T. Devillers, M. Jamet, A. Barski, V. Poydenot, P. Bayle-Guillemaud, E. Bellet-Amalric, S. Cherifi, J. Cibert, Phys. Rev. B 76 (2007), 205306.

[16] Wenguang Zhu, H. H.Weitering, E.G.Wang, Efthimios Kaxiras, and Zhenyu Zhang, Phys. Rev. Lett 93 (2004), 126102.

[17] Changgan Zeng, Zhenyu Zhang, Klaus van Benthem, Matthew F. Chisholm, and Hanno H. Weitering, Phys. Rev. Lett 100 (2004), 066101.

[18] T-G. Le , M-T. Dau, V. Le thanh, D. N. H. Nam, M. Petit, L.A. Michez, N.V. Khiem and M.A. Nguyen, Adv. Nat. Sci.: Nanosci. Nanotechnol. 3 (2012) 025007.

[19] T-G. Le, D.N.H Nam, M-T. Dau, T.K.P Luong, N.V. Khiem, V. Le Thanh, L.A. Michez and J. Derrien, Journal of Physics: Conference Series 292 (2011) 012012.

[20] Thi Giang Le, Minh Tuan Dau, Vinh Le Thanh, Manh An Nguyen, Submited to SPMS – 2013.

[21] Le Thi Giang, Nguyen Manh An, Nguyen Van Hoa, to be published in Proceeding of CASEAN 2013.

[22] Thomas F. Kelly and Michael K. Miller, Invited Review Article: Atom probe tomography, Review of Scientific Instruments 78 (2007), 031101.

[23] C. Zeng, S.C. Erwin, L.C. Feldman, A.P. Li, R. Jin, Y. Song, J.R. Thompson and H.H. Weitering, Appl. Phys. Lett. 83 (2003), 5002.

[24] S.F. Olive-Mendez, A. Spiesser, L.A. Michez, V. Le Thanh, A. Glachant, J. Derrien, T. Devillers, A. Barski, M. Jamet, Thin Solid Films 517 (2008), 191.